On the Leakage Flow around Gas Bubbles in Slug Flow in a Microchannel

Chaoqun Yao, Zhengya Dong, Yuchao Zhang, Yuan Mi, Yuchao Zhao, and Guangwen Chen
Dalian National Laboratory for Clean Energy, Dalian Institute of Chemical Physics, Chinese Academy of Sciences, Dalian 116023, China

DOI 10.1002/aic.14895
Published online June 11, 2015 in Wiley Online Library (wileyonlinelibrary.com)

The leakage flow is that liquid does not push gas bubbles and leaks through the channel corners. This leakage flow was confirmed by tracking particles moving in the liquid film with a double light path method and was quantified by tracking the gas–liquid interface movement. The results show that leakage flow varies during bubble formation process. The average net leakage flow $Q_{net\text{-}leak}$ in a bubble formation cycle at T-junction can be as large as 62.4% of the feeding liquid flow rate, depending on the liquid properties. $Q_{net\text{-}leak}$ for regular flow at main channel is much smaller, ranging from about 0 to 30% of the feeding liquid flow rate. The difference between the two leakage flows would lead to an increase in liquid slug length after generation. Finally, the effects of parameters such as phase flow rates, surface tension, and viscosity were investigated. © 2015 American Institute of Chemical Engineers *AIChE J*, 61: 3964–3972, 2015
Keywords: microreactor, microfluidic, hydrodynamics, multiphase, corner flow

Introduction

Multiphase transport in microchannels or porous media is of significant importance in many areas, such as microchemical engineering,[1,2] on-chip microfluidic analysis,[3,4] oil recovery,[5,6] CO_2 sequestration,[7,8] and fuel cells.[9] At the small scale, interactions between immiscible phases are mainly dominated by surface forces. Therefore, manipulating gas bubbles or liquid droplets in microchannels is much easier than in large scale systems. Up to now, many efforts have been devoted to studying multiphase transport phenomena in microchannels. A common and mostly studied flow pattern is the gas-liquid slug flow, which consists of enlongated gas bubbles and liquid slugs. Uniformly generated gas bubbles and liquid slugs move alternatively in the channel. If the liquid wets the wall, a thin liquid film zone isolates the bubble from contacting channel wall.[10] So gas bubbles are separated from each other while liquid slugs are connected by the liquid film. Such segmented flow can greatly reduce axial back-mixing while enhance radial mixing due to the recirculation pattern in the liquid slugs,[11] which is very beneficial for mass and heat transfer.

Plenty of studies on gas–liquid slug flow have yielded considerable insights into understanding the transport behavior, including bubble formation process,[12–14] bubble shape and liquid film distribution,[10,15,16] pressure drop,[17–19] recirculation,[20,21] and mass transfer.[22–25] Although these studies can provide good guidance for reactor design, there are many problems remaining unsolved and a full understanding of the slug flow characteristics is still rather difficult. Among these problems, an important one is the liquid film flow and its quantification. Liquid film distribution around gas bubbles is strongly affected by channel cross-section. In circular capillaries, thickness of liquid film is usually very thin ($\sim Ca^{2/3}$)[26,27] and cylindrically symmetric. Therefore, film velocity can be neglected as dissipation of mechanical energy is much higher than in the bulk. An enlongated gas bubble acts like a tight-fit piston. In rectangular capillaries, gas bubbles behave as leaky pistons as they do not fill the corners due to surface tension. The liquid that bypasses gas bubble through the corners leads to liquid film flow, which is defined as leakage flow hereafter in this work. Leakage flow is an important parameter that influences bubble formation process,[28] bubble and slug length,[14,15] and bubble velocity.[19,29,30] As to mass transfer, leakage flow can increase the liquid renewal rate in the film, thus, avoiding the ineffectiveness of liquid in the lateral zones of gas bubbles.[31]

There are only a few studies that predict the leakage flow in rectangular microchannels. Fuerstman et al.[19] observed a piece of debris appearing behind and in front of a gas bubble during a sequence of frames, implying some liquid moved through the corners at velocities larger than bubble velocity. They also found that the presence of surfactant can significantly reduce the bubble velocity by up to 50%. Luo and Wang[32] investigated liquid flow pattern around Taylor bubbles using particle tracking method. Their experiments showed that liquid near bubble rear were engulfed into corners and liquid near bubble head were jetted out rapidly. The maximum particle velocities they measured were about 3.6 times larger than the bubble velocities. Kinoshita et al.[33] studied three-dimensional flow field inside water droplets for water–oil segmented flow and found flow near channel wall directed backward while flow near the four corners directed forward in the reference of the

Additional Supporting Information may be found in the online version of this article.

Correspondence concerning this article should be addressed to G. W. Chen at gwchen@dicp.ac.cn

droplets. The results indicated that the immiscible fluids at the two sides of the interfaces can slip freely to some extent, which also shows the continuous phase in the corners flows at a relative large velocity. In fact, the leakage flow had been paid close attention to back in 1995. Wong et al.[26] determined theoretically the leakage flow to scale as $Ca^{-1/3}$ with extremely low Ca and negligible viscosity. Recently, this theory was used to explain the droplet velocities by Jose and Cubaud.[29] Compared to the leakage flow of regular slug flow at main channel, much less research has been focused on the leakage flow during the formation of gas bubbles. van Steijn et al.[13] observed that liquid near bubble interfaces moved into the corners much rapidly during the formation of gas bubble using μ-PIV. Through tracking the interface movement in the squeezing stage, the leakage flow was roughly quantified to be about 10–24% of the feed liquid flow rate. With similar method, we compared the leakage flow at different system pressures and found that the leakage flow rate increases with the increase in system pressure.[14] The above literatures certainly predicted the leakage flow in rectangular microchannels, whereas they also reveal that the leakage flow in the corners has not been directly observed and the quantified information is lacked.

This work aims at improving the understanding of the leakage flow both during the bubble formation process at the junction and during the gas–liquid slug flow at the main microchannel. The leakage flow is qualitatively and quantitatively investigated. The effect of liquid properties on the leakage flow will also be presented.

Experimental

Microfluidic device and experimental setup

The microchannel contactor used in this work was fabricated in a transparent PMMA plate by precision milling (fabrication tolerace: 10 μm) and sealed by another PMMA plate. The inlet configuration of the microchannel is T-shaped junction, as shown in Figure 1. All the channels, including the inlets and main channel, have the same square cross section of 600 μm (width) $\times$ 600 μm (depth). The length of the gas inlet, liquid inlet, and mixing channels are 30 mm, 30 mm, and 60 mm, respectively. Both gas and liquid were delivered by two microsyringe pumps (LSP02-1B, LongerPump). The polyethylene tubes connecting the pumps and inlets have a length of 150 cm and inner diameter of 2.0 mm. Two check valves were used before the gas inlet and liquid inlet, respectively. In this way, pressure fluctuations at the T-junction will not affect the feeding flow rate. The working fluids were air and different aqueous solutions shown in Table 1. The static contact angle θ was measured with an optical measuring device (OCA15, Dataphysics, Germany). All experiments were conducted at atmosphere pressure and room temperature. According to the pressure drop model proposed by Yue et al.,[36] the pressure drop over the entire microchannel reactor varied from 57.3 Pa to 1314.6 Pa, so the compressibility effect of gas could be neglected.

To find direct evidences of leakage flow, an experimental setup was designed to observe the liquid flow in the channel corners. As shown in Figure 1, two light beams were used to lighten the flow pattern. Besides the light source placed below the channel plate, another light source was placed at the side direction. As the interface near the channel corners was curved, the light beam from light 2 could be reflected to the camera lens. This light intensity has to be very strong for only a small fraction of light can be reflected. Polystyrene particles with diameter of about 9 μm were added into 0.14% SDS solution to trace the flow characteristics.

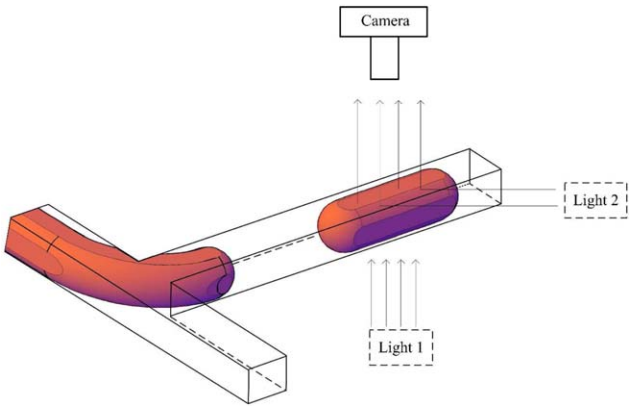

Figure 1. Schematic of the T-junction microchannel.

[Color figure can be viewed in the online issue, which is available at wileyonlinelibrary.com.]

Methodology for quantification of the leakage flow

A cycle of bubble formation includes a filling stage and a squeezing stage. In the filling stage, the bubble tip penetrates into liquid phase and moves forward until contacting the channel wall on the opposite side. During this stage, the channel width is not blocked and liquid can flow through the gap between the bubble and the channel wall with relative ease. In the squeezing stage, the channel width is almost blocked by the growing bubble. So liquid has to flow through the channel corners. This part of liquid flow is defined as the leakage flow. The other part of liquid that does not flow around bubble pushes gas–liquid interface downstream until pinch-off. It is defined as the upstream flow. Continuity of liquid indicates that the feed liquid flow rate (Q_L) equals the plus of the leakage flow rate (Q_{leak}) and upstream flow rate (Q_{up})

$$Q_L = Q_{leak} + Q_{up} \tag{1}$$

Q_{up} can be well estimated from the interface movement due to the squeeze of liquid. As the interface moves forward, the liquid volume upstream of the bubble (V_{up}(t)) increases and instaneous Q_{up} is calculated as dV_{up}/dt. In any period, the average Q_{up} is given by

$$\bar{Q}_{up} = \frac{1}{t_2 - t_1}\int_{t_1}^{t_2} \frac{dV_{up}}{dt} dt = \frac{V_{up}|_{t_2} - V_{up}|_{t_1}}{t_2 - t_1} \tag{2}$$

Accordingly, for a complete formation cycle, the overall mean Q_{up} can be calculated

Table 1. Physical Properties of SDS and Glycerol Solutions at 30°C[34,35]

	SDS content/ wt %			Glycerol content/ wt %		
	0.042	0.087	0.14	5	30	50
ρ/kg m^{-3}	995.6	995.6	995.6	1000.8	1068.7	1120.9
μ/mPa s	0.80	0.80	0.80	0.91	1.87	4.21
σ/mN m^{-1}	62.3	54.9	34.7	70.1	69.2	67.6
θ/°	60	56	53	69	67	65

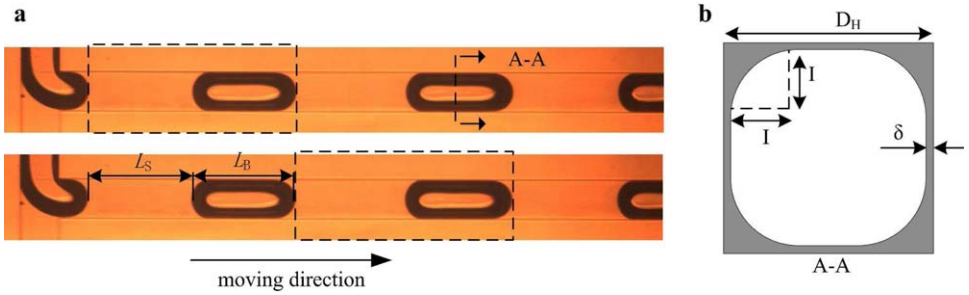

Figure 2. (a) A unit containing a gas and a bubble (b) Cross-section of gas bubble.

[Color figure can be viewed in the online issue, which is available at wileyonlinelibrary.com.]

$$\bar{Q}_{up}=\frac{1}{T}\int_0^T \frac{dV_{up}}{dt}dt=\frac{V_{up}|_T-V_{up}|_0}{T} \quad (3)$$

Actually, this value is the volume of originally generated slug divided by formation period. So it can be simply calculated by

$$\bar{Q}_{up}=\frac{V_{slug}}{T} \quad (4)$$

The leakage flow defined here consists the liquid that flows at the same pace with bubble, so the amount of the net leakage flow that passes bubble is smaller and can be calculated as

$$Q_{net\text{-}leak}=Q_{Leak}-\frac{V_{film}}{T} \quad (5)$$

where V_{film} denotes the volume of liquid film around gas bubbles. Combining Eqs. 1 and 4, Eq. 5 is further written as

$$Q_{net\text{-}leak}=\ Q_L-\frac{V_{slug}+V_{film}}{T} \quad (6)$$

where V_{slug} denotes the volume of liquid slug. This relationship can be better understood with the concept of unit cell shown in Figure 2a. $V_{slug}+V_{film}$ then denotes the total amount of liquid in a unit cell.

To quantify the net leakage flow, it is necessary to know the gas bubble volume. A model of bubble cross section was proposed to estimate them. As shown in Figure 2b, the model assumes that the interface at the corner is a quadrant. The radius of the quadrant can be directly calculated from captured 2-D images as the width of the black area, because the black area was caused by the strong light reflection.[15] The film thickness near the channel wall center was predicted using the correlation from Aussillous and Quéré[27]

$$\frac{\delta}{D_H}=\frac{0.67Ca^{2/3}}{1+3.35Ca^{2/3}} \quad (7)$$

The bubble caps were treated as two hemispheres with a radius of $0.5D_H$-δ. Therefore, the bubble volume can be calculated as

$$V_B=((\pi-4)I^2+(D_H-2\delta)^2)(L_B-D_H)+\frac{4}{3}\pi(0.5D_H-\delta)^3 \quad (8)$$

Then, the net leakage flow was obtained using the following equation

$$Q_{net\text{-}leak}=Q_L-\frac{(L_B+L_S)D_H^2-V_B}{T} \quad (9)$$

The $Q_{net\text{-}leak}$ during bubble formation and at the main channel were calculated when the original and final slug length were used, respectively.

In Figure 3, a typical bubble formation cycle from the squeezing stage to the filling stage was presented. The experiment was conducted using 0.14 wt % SDS solution and air, at a liquid flow rate of 0.3 mL/min and a gas flow rate of 0.6 mL/min. The area marked with green showed how V_{up} at different times in the cycle was calculated. The estimate would be exact

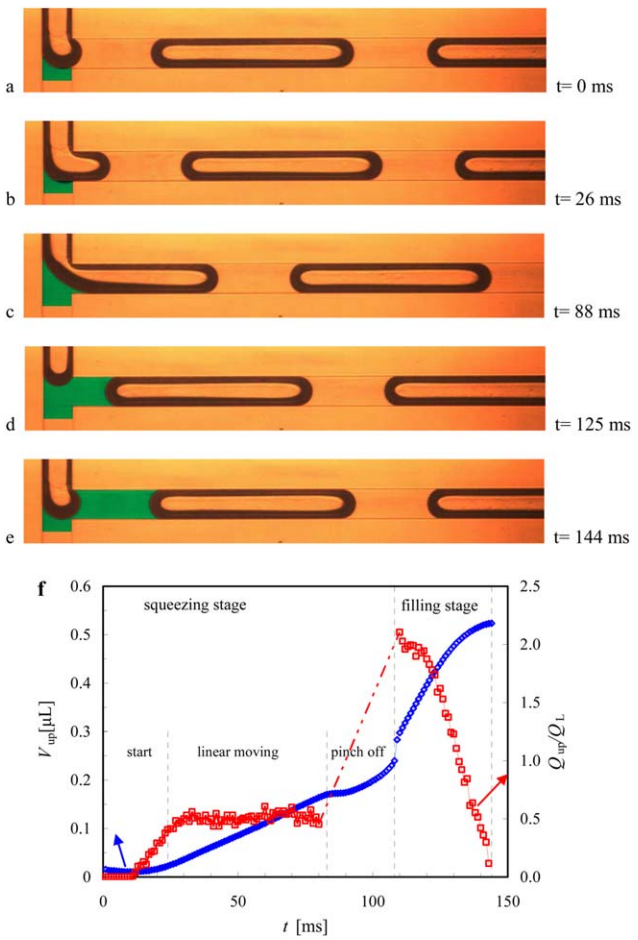

Figure 3. (a)–(e) Photographs of a bubble formation cycle. (f) Evolution of estimated instaneous liquid volume and upstream flow rate Q_{up}/Q_L. $Q_G = 0.6$ mL/min, $Q_L = 0.3$ mL/min, 0.14% SDS solution as liquid phase, $T = 144$ ms.

[Color figure can be viewed in the online issue, which is available at wileyonlinelibrary.com.]

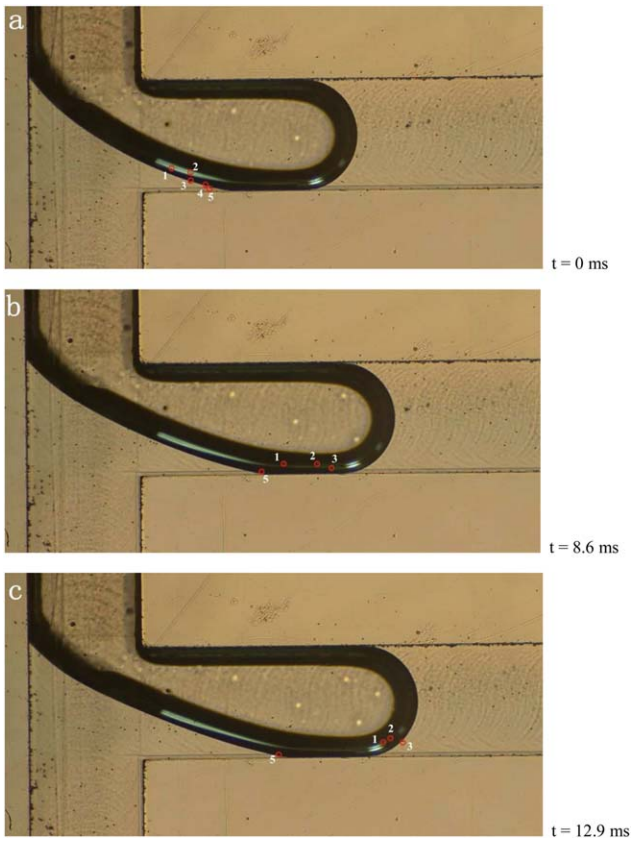

Figure 4. Leakage flow during bubble formation at the T-junction (see video 1 in the Supporting Information).

[Color figure can be viewed in the online issue, which is available at wileyonlinelibrary.com.]

if the bubble curvature in depth-wise direction is constant, which could be speculated from 2-D images for most frames except when the bubble neck shrinks drastically. Instaneous V_{up} and Q_{up}/Q_L were plotted as a function of time in Figure 3f. It can be seen that the evolution pattern is clearly distinguished as two different parts, which correspond to the squeezing and filling stage, respectively. The squeezing stage can further be divided into three substages. The first one is the start of the squeezing stage during which only the bubble tip moves forward after contacting the wall while the bubble neck has the largest width and keeps almost stationary, as shown in Figures 3a, b. As a result, V_{up} also keeps almost constant. In the second substage, the bubble neck is squeezed by the liquid upstream and shrinks gradually. It was observed that V_{up} increases linearly with time. In other words, the instaneous Q_{up} is constant at the stage. However, the instaneous Q_{up} is only about 50% of the feed flow rate Q_L. When the process proceeds into pinch-off stage, the bubble neck shrinks drastically, leading to a sudden jump in Figure 3f. Therefore, the calculation of V_{up} was difficult to determine accurately, thus, Q_{up} was not presented. But it could be deduced that Q_{up} increased drastically during this stage. In the squeezing stage, the blockage of the liquid leads to an increase of pressure ($\sim O(10^2)$ Pa) in the liquid upstream[14,37] and the average Q_{up} is much less than Q_L. In the filling stage, when the bubble neck pinches off, the accumulated pressure is suddenly released and instaneous Q_{up} reaches its maximum value of $2.1Q_L$. Then it keeps decreasing to approximate zero until the bubble tip of next cycle approaches the channel wall.

According to Eq. 2, the overall mean Q_{up} in the squeezing stage was calculated as 0.112 mL/min, which only counted about 37.3% of Q_L. However, the overall mean Q_{up} in the filling stage was much larger than Q_L, which counted about 138.3% of Q_L. The phenomenon suggests much liquid was blocked in the feed line and neither pushed the interface nor leaked through the corners during squeezing stage. Since liquid at atmospheric pressure was nearly incompressible, it may be caused by the fact that the plastic feeding tube was inflated due to increased pressure or the liquid filled some void in the feed line. Therefore, it induces large error to calculate leakage flow if only interface movement in the squeezing stage is included.[13,14] However, for a whole formation cycle, the calculation would be exact because the flow situations at the start and end of the cycle are all the same, as shown in Figures 3a, e. The overall mean Q_{up} was about 0.214 mL/min (71.3% of Q_L), indicating about 28.7% of Q_L leakage flow happened.

Results and Discussion

Evidences of leakage flow at the T-junction and at the main channel

Figure 4 shows tracking of some particles flowing through the channel corners during bubble formation with the double light path method. The bright area in the dark zone was lightened by the side light beam and polystyrene particles moving in the corners could be observed. As can be seen, moving behavior of the particles near gas–liquid interface was rather different from each other.[32] Particles can either move slower or much faster than the bubble tip. These particles with larger velocities were finally sprayed out at different locations in front of the bubble tip. And also, some particles were attached on the interface and thereafter moved at the same pace with the interface. Particle 4 may be one of that kind of particles as its trace disappeared after engulfed in the dark area. The phenomena indicate that there is a large velocity distribution in the corners. The particle velocities were calculated to compare with bubble velocities. Amazingly, the maximum particle velocity observed was about 10 times the bubble velocity, indicating significant amount of liquid passed by the emerging bubble, acting as leakage flow.

Particles moving through the channel corners at the main channel were also observed. Figure 5 shows three polystyrene particles marked with red circles moving at different velocities.

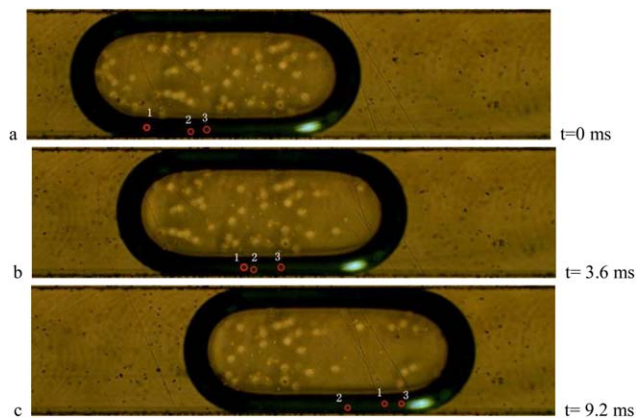

Figure 5. Leakage flow at the main channel (see video 2 in the Supporting Information).

[Color figure can be viewed in the online issue, which is available at wileyonlinelibrary.com.]

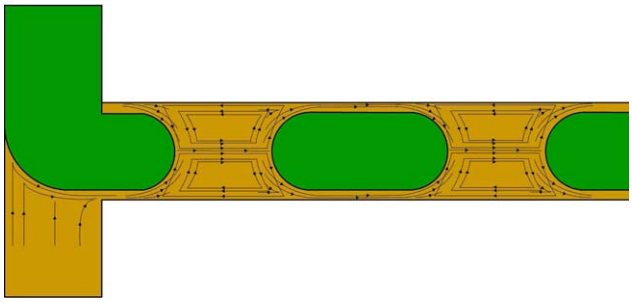

Figure 6. Schematic showing of the recirculation and leakage flow.

[Color figure can be viewed in the online issue, which is available at wileyonlinelibrary.com.]

As can be seen, particle 1 approached and outstripped particle 2 quickly, indicating a large velocity distribution in the corners, too. Interestingly, it was observed that the trajectories of polystyrene particles moving in the corners were always straight. The average velocity of particle 1 was 131 mm/s, which was more than double the bubble velocity (60.6 mm/s). This suggests that there was also a significant amount of leakage flow occurred through the channel corners. It is interesting to note that we conducted similar experiments in a circular quartz capillary, but no obvious moving particles in the film were observed. As the ratio of maximum particle velocity to bubble velocity was larger at the T-junction, one may infer that the leakage flow at T-junction is larger than at main channel.

An important aspect of the leakage flow is related to the fluid transport near the gas–liquid interface. The liquid near the centerline moves faster than the gas bubble. Therefore, they have to change direction when catching up the bubble rear. In the reference frame of the bubble, this turns into recirculation flow.[20,30] Many researches have been devoted to investigating the flow field near bubble interface,[13,20,32,38] but very few related to the leakage flow. According to the particle moving behavior, a sketch of the leakage flow was given in Figure 6, which qualitatively illustrates how neighbor liquid slugs exchange material through leakage flow. Due to the pressure drop over the gas bubble,[28] liquid is engulfed from near bubble rear into the corners and is driven out to the liquid bulk. During this process, the fluid velocity can be several times larger than the bubble cap.[32] After sprayed out, the liquid finally joins the recirculation liquid in the neighbor slug under the push of recirculation. Through this way, exchange of the fluid between neighbor slugs occurs and axial mixing is enhanced.

Another phenomenon also verified that considerable amount of leakage flow bypassed the gas bubble at the T-junction. That is, the liquid slug length still increases a lot after the slug is generated. As shown in Figure 7, the liquid slug length increased more than 100% during the squeezing stage (Figures 7a–d). After the emerging bubble of next cycle completely blocks the channel width, the liquid slug length would then keep constant. This phenomenon verifies the speculation that leakage flow during bubble formation is larger than that at main channel. The degree of increase in the liquid slug length directly shows the difference between the leakage flows at the two locations. When the difference is large, the amount of bypassed liquid during bubble formation cannot be balanced by the leakage flow at the main channel; a part of the liquid

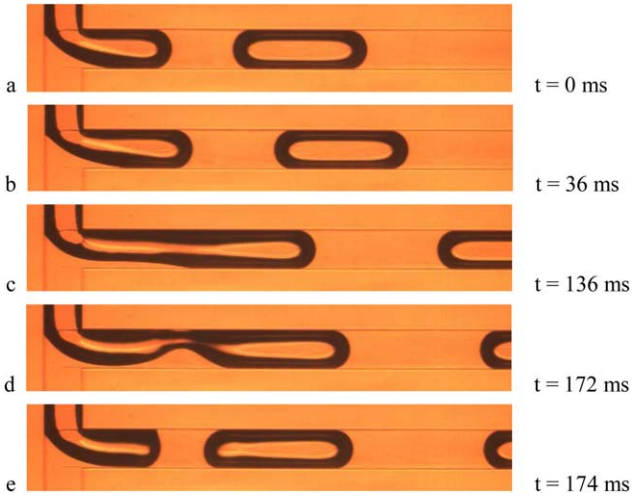

Figure 7. The leakage flow at T-junction leading to increasing of the liquid slug length. $Q_G = 0.3$ mL/min, $Q_L = 0.3$ mL/min, 5% glycerol solution as liquid phase.

[Color figure can be viewed in the online issue, which is available at wileyonlinelibrary.com.]

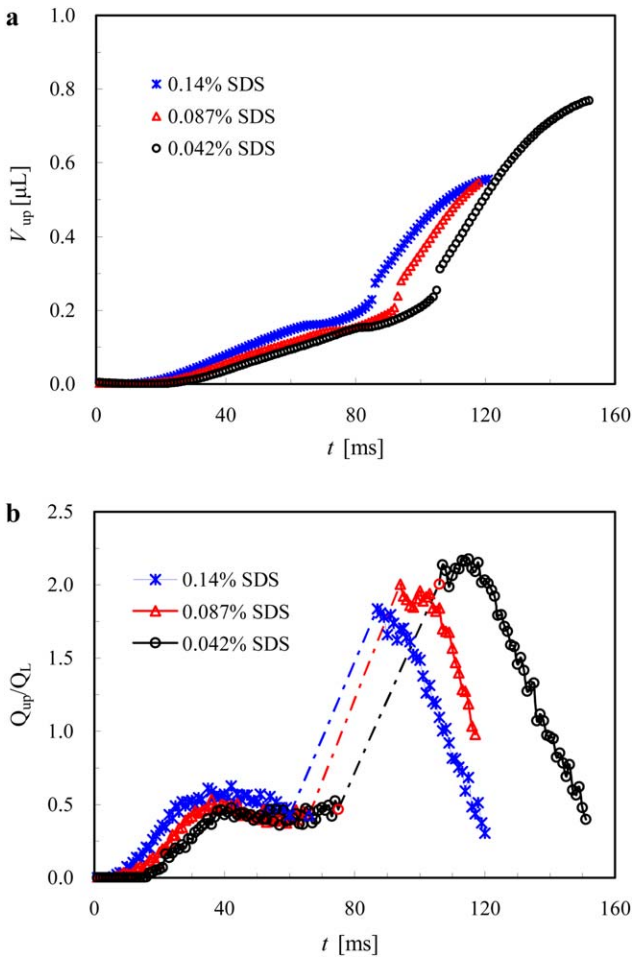

Figure 8. The effect of surfactant concentration on the upstream liquid flow (a) instaneous upstream liquid volume (b) instaneous upstream liquid flow rate. $Q_G = 0.6$ mL/min, $Q_L = 0.4$ mL/min.

[Color figure can be viewed in the online issue, which is available at wileyonlinelibrary.com.]

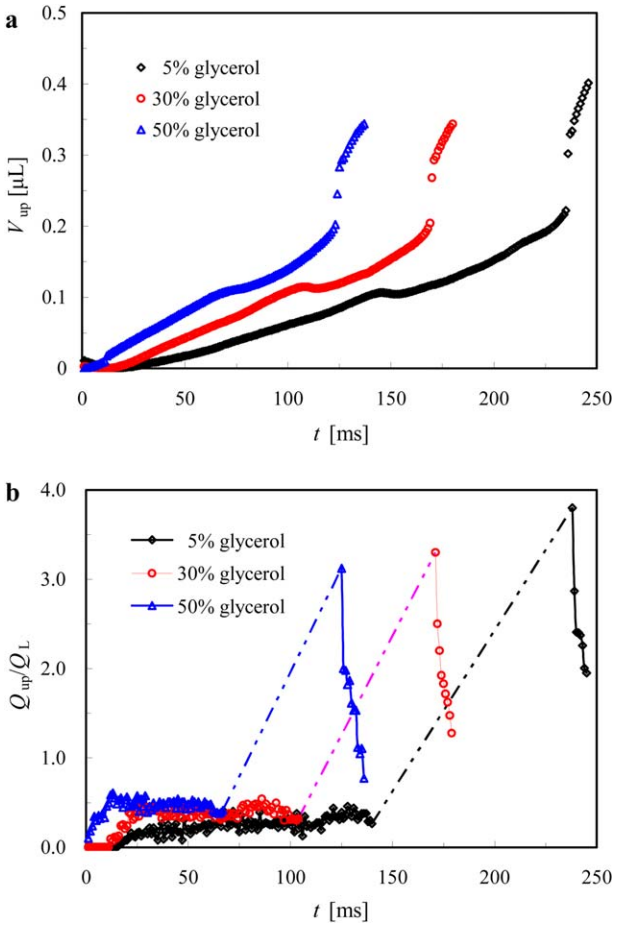

Figure 9. The effect of glycerol concentration on the upstream liquid flow (a) instaneous upstream liquid volume (b) instaneous upstream liquid flow rate. $Q_G = 0.6$ mL/min, $Q_L = 0.2$ mL/min.

[Color figure can be viewed in the online issue, which is available at wileyonlinelibrary.com.]

has to push the bubble forward and generates much longer liquid slug. In this way, the flow fluctuation due to bubble generation is dampened downstream.[39] The mechanism is pretty important for the flow stability in the main channel.

Upstream flow Q_{up} at the T-junction

The effect of viscosity and surface tension on the upstream liquid flow was studied. Sodium dodecyl sulfonate (SDS) and glycerol were used to adjust the surface tension and viscosity, respectively. The physical properties of the solutions used are displayed in Table 1. Figure 8 shows the comparison of the upstream liquid flow with different SDS concentrations. It can be seen that larger Q_{up} in squeezing stage was obtained with higher SDS concentration while smaller Q_{up} in filling stage was obtained. But the difference is relatively small. As to the effect of viscosity, the influence is much larger, as shown in Figure 9. Q_{up} in the squeezing stage increases with the increase in viscosity. However, the difference in Q_{up} in the filling stage is not significant. Another interesting phenomenon is that higher viscosity leads to both shorter start stage and linear moving stage in the squeezing stage, resulting in smaller bubbles.[40] The results here suggest that leakage flow is reduced when liquid is more viscous, as predicted by Wong et al.[26]

Net leakage flow at the T-junction and at the main channel

Figure 10 shows the evolution of the net leakage flow as a function of liquid flow rate for different gas flow rates. The filled symbols represent the net leakage flow during bubble formation at the T-junction and the open symbols represent the net leakage flow for regular slug flow at the main channel. It can be seen that both the two net leakage flows increase with liquid flow rate and decrease with gas flow rate. This is because either higher liquid flow rate or smaller gas flow rate leads to shorter gas bubble which is easier for liquid to bypass. The results also show that the net leakage flow at the T-junction is always larger than that at the main channel. To fulfill the liquid continuity, the length of liquid slugs has to increase for a certain time as discussed above. For 5% glycerol, the net leakage flow at T-junction occupies about 17.1–62.4% of the feeding liquid flow, whereas at main channel it is only about 3.3–18.3%, as shown in Figure 10a. The difference between the two leakage flows is very large, leading to a large relative increase in liquid slug length ($\Delta L_S/L_{S0}$). For 0.14% SDS solution, the two leakage flows range from 7.9% to 42.5% and 6.0% to 30.0% of the feeding liquid flow,

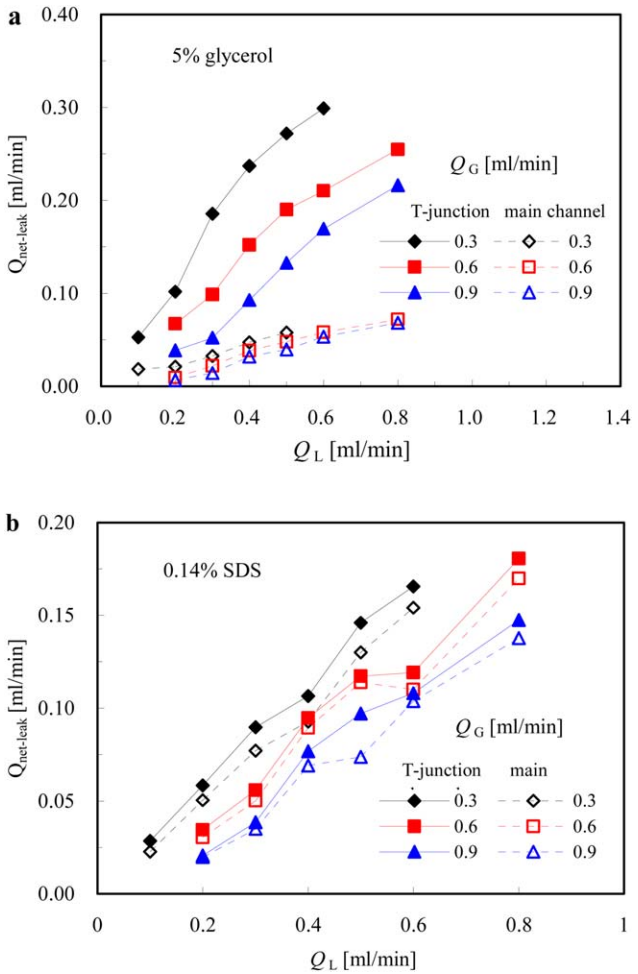

Figure 10. The effect of flow rates on the net leakage flow during bubble formation at the T-junction and for regular slug flow at the main channel.

[Color figure can be viewed in the online issue, which is available at wileyonlinelibrary.com.]

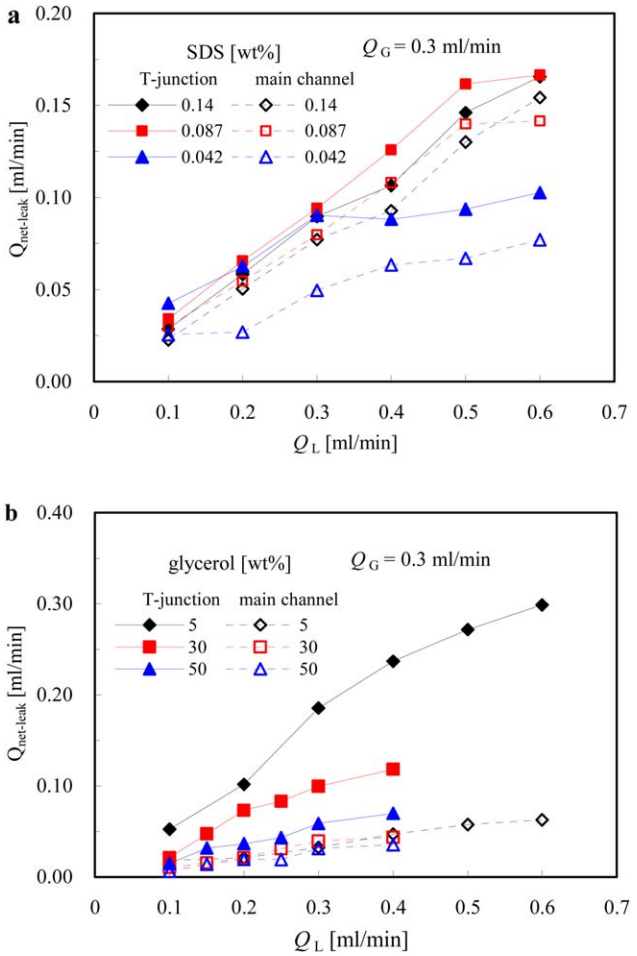

Figure 11. The effect of (a) surfactant concentration and (b) glycerol concentration on the net leakage flow at the T-junction and at the main channel.

[Color figure can be viewed in the online issue, which is available at wileyonlinelibrary.com.]

respectively. The difference between the two leakage flows is much smaller.

From Figure 11a, it can be seen that higher surfactant concentration can lead to larger net leakage flow. The net leakage flow firstly increases rapidly and then increases a little when SDS concentration is added from 0.042% to 0.014%. For surfactant concentration, there are two antagonistic effects. As the pressure drop across a gas bubble is the main drive for the leakage flow,[28] lower surface tension is obtained with higher surfactant concentration and then reduces the leakage flow.[26] Conversely, large amount of surfactant molecules adsorbed on the gas–liquid interface make the interface more rigid. This may be beneficial for leakage flow, as observed by Fuerstman et al.[19] It seems that the latter factor should be dominant in the experiments, leading to the results shown in Figure 11a.

Figure 11b shows the effect of viscosity on the net leakage flow. Since the corners are affected by larger viscous forces than channel center regions,[6] the effect of increasing liquid viscosity on the flow resistance of leakage flow is larger. Therefore, increasing glycerol concentration can significantly reduce the leakage flow. For different glycerol solutions, the net leakage flow at main channel is always very small and the effect of glycerol concentration is not obvious, as shown in Figure 11b.

From Figure 11, it can also be seen that both higher SDS and glycerol concentration will reduce the difference between the two leakages at the T-junction and at main channel. But the mechanisms are different. Increasing SDS concentration increases both the two leakage flows and the leakage flow at main channel increases at a larger content. On the contrary, the leakage flow at T-junction decreases more than at main channel when increasing glycerol concentration. Generally, the difference between the two net leakage flows for SDS solutions is smaller than for glycerol solutions under experimental conditions.

The effect of leakage flow on liquid slug length

As stated before, the leakage flow at T-junction is always larger than that at main channel. Therefore, the liquid slug length will always increase after the slug is generated. The influence of leakage flow on the slug length increase can be observed by plotting the relative increase of liquid slug length $\Delta L_S/L_{S0}$ vs. the difference between the two leakage flows $\Delta Q_{net\text{-}leak}/Q_L$. The results are shown in Figure 12. As can be seen, two regions are identified. Region-1 happens when the channel wall at T-junction is well wetted. The bubble neck ruptures right at the T-junction and then the bubble tip retreats back to the gas inlet channel, which can be more clearly seen in Figure 3. In this region, $\Delta Q_{net\text{-}leak}/Q_L$ is smaller than 25% and the corresponding $\Delta L_S/L_{S0}$ increases slowly with $\Delta Q_{net\text{-}leak}/Q_L$. Region-2 happens when the channel wall at T-junction is poorly wetted. $\Delta Q_{net\text{-}leak}/Q_L$ is much higher and $\Delta L_S/L_{S0}$ increases rapidly. For poorly wetted condition, the bubble neck ruptures at downstream the T-junction. The new bubble cap has a tendency to adhere to channel wall surfaces and does not retreat back, as shown in Figure 7. Similar observation was reported by Jose and Cubaud[29] recently. It is much more difficult for upstream liquid to push the emerging bubble to move forward since it has to scrape the liquid attached to the channel wall. Then upstream liquid has to leak through the corners, leading to very large $\Delta L_S/L_{S0}$. In the present study, the very poor wetting condition at T-junction is a metastable state and only occurred with 5% glycerol solution at very small flow rates. Increasing gas or liquid flow rates, glycerol concentration, and SDS concentration would largely improve the wetting condition.

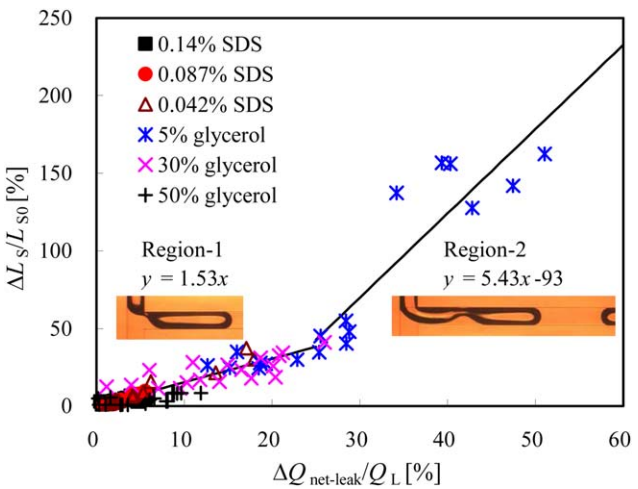

Figure 12. The effect of leakage flow on the liquid slug length increase.

[Color figure can be viewed in the online issue, which is available at wileyonlinelibrary.com.]

Conclusion

In a square microchannel, the bubble surface cannot fill all the corners due to surface tension so the gas bubble acts like a leaky piston. Leakage flow is the flow of liquid through the channel corners, which is of significant importance to the flow and mass transfer of slug flow. This work has focused on the leakage flow at the T-junction for bubble formation and at main channel for regular flow. The leakage flow was confirmed by particle experiments with a double light path method and quantification of the leakage flow was obtained with 2-D captured flow images. Main findings and conclusions are presented as following:

1. Polystyrene particles flowing through corners between gas bubble and channel walls moved at different velocities, indicating large velocity distribution in the liquid film. At the T-junction, the maximum particle velocity can be as large as 10 times the bubble cap velocity. At the main channel, particles with velocity 2 times larger than the bubble velocity were also observed.

2. The squeezing stage of bubble formation can be divided into three sub-stages. The first one is the start stage during which upstream liquid flow is nearly zero. The second one is the linear moving stage when the upstream liquid flow is constant. The last one is the shrinkage stage during which bubble neck shrinks rapidly and the upstream liquid flow increases a lot. This shows that the leakage flow varies during bubble formation.

3. SDS concentration and glycerol concentration have large influences on the upstream flow. Higher SDS concentration leads to larger upstream flow in the squeezing stage while leads to smaller one in the filling stage. Higher glycerol concentration or viscosity leads to larger upstream flow in the squeezing stage while has no significant impact on that in the filling stage.

4. The two net leakage flows were quantified based on a bubble shape model. The average net leakage flow $Q_{\text{net-leak}}$ in a bubble formation cycle at the T-junction can be as large as 62.4% of the feeding liquid flow rate, depending on the liquid properties. $Q_{\text{net-leak}}$ at the main channel is much smaller, ranging from about 0 to 30% of the feeding liquid flow rate. Both the two leakage flows increase with the increase in liquid flow rate, whereas decrease with the increase in gas flow rate. Higher SDS concentration and smaller glycerol concentration are beneficial for leakage flow.

5. Net leakage flow at the T-junction for bubble formation is larger than at the main channel for regular flow. This leads to increase in the liquid slug length after the slug is generated. When the channel wall is not well wetted at the T-junction, the net leakage flow is much higher, leading to much more increase in the slug length. Under some conditions in the experiments, $\Delta L_S/L_{S0}$ can be as large as 170%.

Acknowledgments

We acknowledge gratefully the financial supports for this project from National Natural Science Foundation of China (Nos. 21225627, 21376234).

Notation

Ca = two phase capillary number defined by ($=\mu_L j_{TP}/\sigma_L$)
D_H = hydrodynamic diameter
H = depth of the microchannel
L = length
Q = flow rate
T = bubble formation period
t = time
V = volume

Subscripts

B = bubble
G = gas
L = liquid
S = liquid slug
S0 = original liquid slug
up = upstream

Literature Cited

1. Yue J, Chen GW, Yuan Q, Luo L, Gonthier Y. Hydrodynamics and mass transfer characteristics in gas–liquid flow through a rectangular microchannel. *Chem Eng Sci*. 2007;62(7):2096–2108.
2. Jensen KF. Microreaction engineering—is small better? *Chem Eng Sci*. 2001;56(2):293–303.
3. Yue J, Schouten JC, Nijhuis TA. Integration of microreactors with spectroscopic detection for online reaction monitoring and catalyst characterization. *Ind Eng Chem Res*. 2012;51(45):14583–14609.
4. El-Ali J, Sorger PK, Jensen KF. Cells on chips. *Nature*. 2006; 442(7101):403–411.
5. Foroughi H, Abbasi A, Das KS, Kawaji M. Immiscible displacement of oil by water in a microchannel: asymmetric flow behavior and nonlinear stability analysis of core-annular flow. *Phys Rev E*. 2012; 85(2):10.
6. Kolb WB, Cerro RL. Coating the inside of a capillary of square cross-section. *Chem Eng Sci*. 1991;46(9):2181–2195.
7. Voicu D, Abolhasani M, Choueiri R, Lestari G, Seiler C, Menard G, Greener J, Guenther A, Stephan DW, Kumacheva E. Microfluidic studies of CO_2 sequestration by frustrated Lewis pairs. *J Am Chem Soc*. 2014;136(10):3875–3880.
8. Sun R, Cubaud T. Dissolution of carbon dioxide bubbles and microfluidic multiphase flows. *Lab Chip*. 2011;11(17):2924–2928.
9. Litster S, Sinton D, Djilali N. Ex situ visualization of liquid water transport in PEM fuel cell gas diffusion layers. *J Power Sources*. 2006;154(1):95–105.
10. Fries DM, Trachsel F, von Rohr PR. Segmented gas–liquid flow characterization in rectangular microchannels. *Int J Multiphase Flow*. 2008;34(12):1108–1118.
11. Gunther A, Jhunjhunwala M, Thalmann M, Schmidt MA, Jensen KF. Micromixing of miscible liquids in segmented gas-liquid flow. *Langmuir*. 2005;21(4):1547–1555.
12. Garstecki P, Fuerstman MJ, Stone HA, Whitesides GM. Formation of droplets and bubbles in a microfluidic T-junction-scaling and mechanism of break-up. *Lab Chip*. 2006;6(3):437–446.
13. van Steijn V, Kreutzer MT, Kleijn CR. μ-PIV study of the formation of segmented flow in microfluidic T-junctions. *Chem Eng Sci*. 2007; 62(24):7505–7514.
14. Yao CQ, Dong ZY, Zhao YC, Chen GW. The effect of system pressure on gas-liquid slug flow in a microchannel. *AIChE J*. 2014; 60:1132–1142.
15. Yao CQ, Zhao YC, Ye CB, Dang MH, Dong ZY, Chen GW. Characteristics of slug flow with inertial effects in a rectangular microchannel. *Chem Eng Sci*. 2013;95:246–256.
16. Han Y, Shikazono N. Measurement of liquid film thickness in micro square channel. *Int J Multiphase Flow*. 2009;35(10):896–903.
17. Yue J, Luo L, Gonthier Y, Chen GW, Yuan Q. An experimental investigation of gas–liquid two-phase flow in single microchannel contactors. *Chem Eng Sci*. 2008;63(16):4189–4202.
18. Kreutzer MT, van der Eijnden MG, Kapteijn F, Moulijn JA, Heiszwolf JJ. The pressure drop experiment to determine slug lengths in multiphase monoliths. *Catal Today*. 2005;105(3–4):667–672.
19. Fuerstman MJ, Lai A, Thurlow ME, Shevkoplyas SS, Stone HA, Whitesides GM. The pressure drop along rectangular microchannels containing bubbles. *Lab Chip*. 2007;7(11):1479–1489.
20. Zaloha P, Kristal J, Jiricny V, Völkel N, Xuereb C, Aubin J. Characteristics of liquid slugs in gas–liquid Taylor flow in microchannels. *Chem Eng Sci*. 2012;68(1):640–649.

21. Waelchli S, Rudolf von Rohr P. Two-phase flow characteristics in gas–liquid microreactors. *Int J Multiphase Flow*. 2006;32(7):791–806.
22. Yue J, Luo L, Gonthier Y, Chen GW, Yuan Q. An experimental study of air–water Taylor flow and mass transfer inside square microchannels. *Chem Eng Sci*. 2009;64(16):3697–3708.
23. Yao CQ, Dong ZY, Zhao YC, Chen GW. An online method to measure mass transfer of slug flow in a microchannel. *Chem Eng Sci*. 2014;112:15–24.
24. van Baten JM, Krishna R. CFD simulations of mass transfer from Taylor bubbles rising in circular capillaries. *Chem Eng Sci*. 2004; 59(12):2535–2545.
25. Yao CQ, Dong ZY, Zhao YC, Chen GW. Gas-liquid flow and mass transfer in a microchannel under elevated pressures. *Chem Eng Sci*. 2015;123:137–145.
26. Wong H, Radke CJ, Morris S. The motion of long bubbles in polygonal capillaries. Part 2. Drag, fluid pressure and fluid flow. *J Fluid Mech*. 1995;292:95–100.
27. Aussillous P, Quéré D. Quick deposition of a fluid on the wall of a tube. *Phys Fluids*. 2000;12(10):2367–2371.
28. van Steijn V, Kleijn CR, Kreutzer MT. Flows around confined bubbles and their importance in triggering pinch-off. *Phys Rev Lett*. 2009;103(21):214501(1)–204501(4).
29. Jose BM, Cubaud T. Formation and dynamics of partially wetting droplets in square microchannels. *RSC Adv*. 2014;4(29):14962–14970.
30. Baroud CN, Gallaire F, Dangla R. Dynamics of microfluidic droplets. *Lab Chip*. 2010;10(16):2032.
31. Pohorecki R. Effectiveness of interfacial area for mass transfer in two-phase flow in microreactors. *Chem Eng Sci*. 2007;62(22):6495–6498.
32. Luo R, Wang L. Liquid flow pattern around Taylor bubbles in an etched rectangular microchannel. *Chem Eng Res Des*. 2012;90(8):998–1010.
33. Kinoshita H, Kaneda S, Fujii T, Oshima M. Three-dimensional measurement and visualization of internal flow of a moving droplet using confocal micro-PIV. *Lab Chip*. 2007;7(3):338–346.
34. Hernźinz F, Caro A. Variation of surface tension in aqueous solutions of sodium dodecyl sulfate in the flotation bath. *Colloids Surf A Physicochem Eng Asp*. 2002;196:19–24.
35. Oberstak Jbsahe. Viscosity of glycerol and its aqueous solutions. *Ind Eng Chem*. 1951;43:2117–2120.
36. Yue J, Rebrov EV, Schouten JC. Gas-liquid-liquid three-phase flow pattern and pressure drop in a microfluidic chip: similarities with gas-liquid/liquid-liquid flows. *Lab Chip*. 2014;14(9):1632–1649.
37. Li XB, Li FC, Yang JC, Kinoshita H, Oishi M, Oshima M. Study on the mechanism of droplet formation in T-junction microchannel. *Chem Eng Sci*. 2012;69(1):340–351.
38. Fries D, Waelchli S, Rudolfvonrohr P. Gas–liquid two-phase flow in meandering microchannels. *Chem Eng J*. 2008;135:S37–S45.
39. Abate AR, Mary P, van Steijn V, Weitz DA. Experimental validation of plugging during drop formation in a T-junction. *Lab Chip*. 2012;12(8):1516–1521.
40. Dang MH, Yue J, Chen GW, Yuan Q. Formation characteristics of Taylor bubbles in a microchannel with a converging shape mixing junction. *Chem Eng J*. 2013;223:99–109.

Manuscript received Mar. 19, 2015, and revision received May 7, 2015.